

SELECTION OF BIOREACTOR MEDIA FOR ODOR CONTROL

Rakesh Govind* and Sandeep Narayan
Department of Chemical Engineering
Mail Location 171
University of Cincinnati
Cincinnati, OH 45221-0171
Tel: (513) 673 3583
Fax: (513) 556 3473 (attn: Govind)
Email: rgovind@alpha.che.uc.edu

Chapter submitted to “*Biotechnology for Odour and Air Pollution Control*”.

***All correspondence concerning this chapter should be addressed to
Dr. Rakesh Govind**

1. Introduction

The support media is one of the most critical elements of a biofiltration system. In this chapter, biofilters and biotrickling filters will be referred to as “biofilter”, and this distinction will be discussed later in this chapter. The support media’s main function is to provide contact between the gas-phase contaminants and active microbial cultures either immobilized within and/or attached as a biofilm on the media’s surface. Other functions of the media are to distribute the gas flow evenly within the bed’s cross-sectional area with minimal gas-phase pressure drop, distribute any liquid nutrients sprayed on the bed’s surface, and prevent accumulation of biomass to prevent clogging, which would eventually lead to channeling of the gas and liquid.

Biofilter media can be classified based on its mass-transfer mechanism, and then sub-classified according to other characteristics, as listed below:

1. Diffusive: contaminants diffuse towards and into the media perpendicular to the gas flow.
 - 1.1 Naturally Bioactive
 - 1.2 Synthetic
 - 1.2.1 Randomly packed
 - 1.2.1.1 Adsorbing
 - 1.2.1.2 Non-Adsorbing
 - 1.2.2 Structured
 - 1.2.2.1 Adsorbing
 - 1.2.2.2 Non-Adsorbing
 - 1.3 Synthetic Encapsulating
 - 1.4 Membrane Systems (Flat sheet, hollow fibers)
2. Convective: contaminants and gas flow through the biofilm and media.

2. Diffusive versus Convective Media

Figure 1 shows the main differences between diffusive and convective biofilter support media. In diffusive media (Figures 1a, 1b), the contaminants in the gas phase diffuse towards and/or into the media, containing immobilized active microbial cultures. The support media itself is not porous and does not allow any gas flow through the media. The diffusive flux of the contaminant is perpendicular to the direction of gas flow, and its value depends on the concentration difference between the bulk and the contaminant concentration at the surface of the gas-biofilm interface. This transport rate is dependant on the gas velocity, and in the case of porous media, there is a combination of film and pore diffusion. An effectiveness factor can be used to describe the effect of diffusion, and can be written as:

$$\eta = \frac{r_{observed}}{r_{bulkconditions}} \quad (1)$$

where $r_{observed}$ = actual measured reaction rate and $r_{bulkconditions}$ = reaction rate at bulk gas conditions. In the case of non-adsorbing media (Figure 1a), there is no adsorbed concentration of the contaminant on the media's surface. However, if the support media adsorbs the contaminant, present in the gas phase, since adsorption is much faster than biodegradation, there is a finite concentration of contaminant on the media's surface, which results in back-diffusion of the contaminant (desorption) into the biofilm, as shown by the concentration profiles in Figure 1b. While the thickness of biofilm in the case of non-adsorbing media is self-limiting (maximum effective biofilm thickness), there is no such thickness in the case of adsorbing media. The mathematics of these differences in concentration profile will be discussed later. However, it should be noted, that as the bulk contaminant concentration decreases, as in the case of odor biofiltration (contaminant concentration is usually low, combined with low Detection and Recognition threshold concentrations), the diffusive flux of the contaminant also decreases, which results in low biofiltration treatment rates. Also, with increasing gas velocity, the diffusive fluxes increase, due to higher mass transfer coefficients.

In the case of convective media (Figure 1c), the biofilm is supported by a porous support media, and the contaminant is carried into the biofilm by convective transport, i.e., actual gas flow, rather than by diffusion only, as in the case of diffusive biomed. Since convective rates are significantly higher than diffusive fluxes, the rate of biofiltration treatment is consequently higher, and is not impacted by bulk contaminant concentrations. Of course, in convective systems, the gas has to flow from the feed side to the product side through the porous biofilm and support media. The effect of adsorbing versus non-adsorbing is the same, namely, that in the case of adsorbing, there is a finite back-diffusion into the biofilm, while there is no such back-diffusion in the case of non-adsorbing media. Clearly, convective biomed, which uses membranes or porous supports, offers higher biofiltration rates, especially at low bulk contaminant concentrations, as in the case of odor control. The need for convective biomed is evident from close examination of a biofilm, as shown in Figure 2. Diffusion of the contaminant occurs from the gas phase into the active biofilm, where simultaneous biodegradation and diffusion occurs. Mathematically, this can be written as follows:

$$\frac{\partial^2 y}{\partial x^2} = \frac{\alpha y}{1 + y} \quad (2)$$

$$\frac{dy}{dx} = 0, \text{ at } x = 0 \quad (3)$$

$$y = y_1, \text{ at } x = 1 \quad (4)$$

where the dimensionless variables and parameters are defined as follows:

$$y = \frac{C_b}{K_C} \quad (5)$$

$$x = \frac{z}{L_b} \quad (6)$$

$$\alpha = L_b^2 \frac{k}{K_C D_{Biofilm}} \quad (7)$$

$$y_1 = \frac{C_{bi}}{K_C} \quad (8)$$

In terms of these dimensionless variables, the effectiveness factor, defined in equation (1) becomes:

$$\eta = \frac{(dy/dx)_{x=1}}{\alpha y_1 / (1 + y_1)} \quad (9)$$

A plot of this effectiveness factor, η , versus the dimensionless concentration at the air/biofilm interface, y_1 , and the Thiele's Modulus ($\sqrt{\alpha}$) is shown in Figure 3. The effectiveness factor becomes significantly less than 1, when either the biofilm is thick, i.e., L_b is large, or the contaminant concentration at the air/biofilm interface is small, i.e., y_1 is small. Under these conditions, diffusive support media becomes ineffective, and use of convective support media increases the biotreatment rates in the biofilter.

3. Naturally Bioactive Media

Naturally bioactive media consist of media, such as soil, compost, peat, cow manure, etc., which naturally contain bacteria dispersed within the structure of the media itself, rather than as a distinct biofilm on the surface and within the pores. Most natural media contain clay and organic matter and adsorption of contaminants on these materials occurs through various interactions, such as van der Waals' forces, H-bonding, dipole-dipole interaction, ion exchange, covalent bonding, ligand exchange, water bridging, and/or hydrophobic partitioning. The organic matter occurs primarily as amorphous gel-like phases that allow for hydrophobic organic compound partitioning (Chiou et al. 1983; Karickhoff et al. 1979). The total sorption of the contaminant can be written as a combination of two mechanisms: (1) Hydrophobic partitioning from the aqueous phase, in which the contaminant has solubilized from the gas phase; and (2) adsorption on the media's surface, that tends to dominate at low contaminant concentrations.

$$q(C) = q_p(C) + q_{ad}(C) \quad (10)$$

Such models have been referred to as "distributed reactivity" (Weber et al. 1999), "dual-mode" sorption (Xing and Pignatello 2001) or simply "adsorption-partitioning" (Accardi-Dey and Hschwend 2002; Chiou

et al. 2000). Hydrophobic partitioning of non-polar contaminants by amorphous organic mater is usually written as a partitioning constant:

$$K_d = \frac{q_p(C)}{C} \quad (11)$$

K_d can also be normalized by the fraction of organic carbon in the media (f_{OC}):

$$K_{OC} = \frac{K_d}{f_{OC}} \quad (12)$$

Empirical regressions between contaminant properties (aqueous solubility (S), octanol-water partitioning coefficient (K_{OW}) provide an effective method for estimating K_{OC} value for a non-polar chemical in naturally bioactive media (Seth et al. 1999; Xia 1998; Gao et al. 1996).

Adsorption on the media's surface can be described by standard adsorption isotherms and are usually derived from the Polanyi adsorption potential for gas-phase adsorption (Polanyi 1916):

$$\varepsilon_d = RT \ln \left(\frac{P^o}{P} \right) \quad (13)$$

where ε_d is the differential work of adsorption, P/P^o is the partial pressure, T is the temperature and R the ideal gas constant. At low gas-phase concentrations, as in odor biofiltration, adsorption dominates the overall sorption process. As originally proposed by Dubinin and Ashtakhov (1971), the adsorbed volume of contaminant (q') can be written as follows:

$$\frac{q'}{q'_{max}} = \exp \left[- \left(\frac{RT \ln(P^o / P)}{\beta_i E_o} \right)^d \right] \quad (14)$$

where q'_{max} is the maximum sorption capacity, the exponent d is a fitting parameter of the characteristic curve, and $\beta_i E_o$ is the characteristic energy of adsorption.

Contaminants, once adsorbed into the organic fraction of the natural media, undergo a combination of abiotic transformations, such as hydrolysis, chemical binding (Ramani and Govind, 2002), redox reactions, polymerization, often catalyzed by the clays and metal oxides present, and microbial breakdown due to aerobic and anaerobic biodegradation primarily by the heterotrophic bacteria and actinomycetes, certain autotrophic bacteria, fungi and specific protozoa.

Mass transfer of the contaminants into the aggregates of the natural media, composed of smaller particles, impacts the performance of the media in biofiltration, and is dependant on the water content of the media, as shown in Figure 4. Below a specific critical water content (W_i in Figure 4), the bioactivity of the media is negligible, and the media loses its structure, developing cracks through which the gas can by-pass the bed. Experiments have shown (Zhao and Govind 1997) that this critical water content in the case of compost, peat, and soil, is an irreversible phenomenon, whereby once the media goes below this

water content, it does not recover its original bioactivity and structure, even if the water content is increased above this critical value. There is an “optimum” water content (maximum bioactivity; W_p in Figure 4), above which the rate of biodegradation begins to decrease mainly due to mass transfer constraints arising from a distinct water film outside the media aggregates.

Naturally bioactive media, such as soils, compost, peat, etc. have a specific water retention capacity due to their inherent porosity, which depends on the media characteristics. While small pores in the support media cannot accommodate biofilms, they can retain water that can be used by the biofilms attached to the media surface, thereby preventing drying of the active biofilms. Materials with significant water retention capacity can be used as biofilter media with humidified air, which reduces water evaporative losses. Usually, for biodegradative activity in naturally bioactive media, moisture content should be in the range of 50-80% of the water holding capacity, which is equivalent to the “field-capacity” (percentage of water remaining in the media after it has been saturated and gravitational drainage has ceased). The water holding capacity is a function of the matric potential (measure of energy required to overcome capillary and adsorptive forces) of the media-water and depends on the organic content of the naturally bioactive media. A matric potential of -0.1 bar or greater is considered optimal for microbial activity in soils.

Table 1 summarizes the model equations that have been developed (Zhao and Govind 1997) to mathematically describe the performance of naturally bioactive media in biofiltration applications. The main advantages and disadvantages of using naturally bioactive media in biofiltration applications are summarized in Table 2.

4. Synthetic Media

Synthetic media consists of structures in which the active bacteria have to be inoculated and are not present inherent in the media’s structure, as in the case of naturally bioactive media. Although synthetic media can be classified according to their structure, shape, size, etc., a more fundamental classification system would be based on their surface characteristics, rather than their geometry.

There are several types of synthetic support media that have been used in biofiltration systems. Synthetic media can be broadly classified as one of two types: (1) adsorbing, which exhibit significant physical adsorption of the contaminant(s); and (2) non-adsorbing, where there is negligible physical adsorption of the contaminants by the media. The major difference between adsorbing and non-adsorbing media is the occurrence of maximum effective biofilm thickness in non-adsorbing media but not in adsorbing media (Govind 2002). In non-adsorbing media, the concentration profile, assuming maximum biofilm thickness, is shown in Figure 3a, where the contaminant concentration at the biofilm-support media interface is zero. Since the contaminant cannot diffuse beyond this maximum biofilm thickness,

any biofilm beyond this depth will begin to decay, eventually resulting in slough-off of the biofilm from the media surface. However, if the contaminant adsorbs on the support media's surface, back-diffusion of the contaminant from the media's surface into the biofilm at the biofilm-support media interface, as shown in Figure 3b, prevents any such limitation of thickness from occurring, resulting in thicker biofilms. The impact of this back-diffusion is increased rates of biofiltration, mainly due to a combination of adsorption-desorption and biodegradation within the biofilm resulting in increased amounts of active biomass within the biofilter. It should be noted that this increase in biofiltration rates is only observed when the contaminant can desorb effectively from the support media and is not irreversibly adsorbed on the surface. Table 3 summarizes the advantages and disadvantages of various types of synthetic media that have been used in biofiltration.

Other important surface characteristics of the support media are surface roughness and charge. It was noticed that the extent of microbial colonization increased with surface roughness (Characklis et al. 1990). This is mainly due to diminished shear forces and increased surface area of the rough surface. Most investigators have found that microorganisms attach more rapidly to hydrophobic, non-polar surfaces than to hydrophilic materials (Fletcher et al. 1979; Pringle and Fletcher 1983; Bendinger et al. 1993). Hydrophobic interaction between the cell's surface and the media's surface enables the cell to overcome the repulsive forces active within a certain distance from the media's surface. Most bacteria are negatively charged, but still contain hydrophobic components on the surface (Rosenberg and Kjelleberg 1986).

However, any material surface exposed in an aqueous medium will inevitably and almost immediately become conditioned or coated by polymers present in the medium, and this resulting chemical modification affects the rate and extent of microbial attachment. Such conditioning films were first reported by Loeb and Neihof (1975). Other characteristics of the aqueous medium that are important for biofilm growth on the media are pH, nutrient levels, ionic strength, and temperature. Fletcher (1988a; 1988b) found that an increase in the concentration of several cations, such as sodium, calcium, ferric ion, increased the attachment of cells to glass surfaces by reducing the repulsive forces between the negatively charged bacterial cells and the glass surface. Cowan et al. (1991) showed that an increase in the nutrient concentration correlated with increases in the number of attached bacterial cells.

The hydrodynamics of liquid flow within the biofilter affects the slough-off of biomass from the support media's surface. The relationship between the rate of shear loss of biofilm ($R_{Slough-off}$) and the biofilm thickness is given by Rittman (1989) as follows:

$$R_{Slough-off} = 3.62 \times 10^{-6} X_f L_f \left[\frac{\tau_s}{1 + 0.0443(L_f - 30)} \right]^{0.58} \text{ when } L_f > 30 \text{ } \mu\text{m} \quad (15)$$

$$= 3.62 \times 10^{-6} X_f L_f \tau_s^{0.58} \quad \text{when } L_f < 30 \text{ } \mu\text{m} \quad (16)$$

where $R_{Slough-off}$ is the rate of biomass slough-off from the media's surface ($\text{kg} \cdot \text{m}^{-2} \cdot \text{s}^{-1}$); τ_s is the shear stress on the biofilm surface due to liquid flow ($\text{N} \cdot \text{m}^{-2}$); L_f is the biofilm thickness in μm ; and X_f is the biofilm density (kg/m^3). Assuming flow occurs over a vertical plate, with only 40% of the available media's surface area covered by the nutrient flow, a bed height of 3 ft, and a media surface area of $100 \text{ ft}^2/\text{ft}^3$, we get the following result for the biomass slough-off rate:

$$R_{Slough-off} = 2.9 \times 10^{-7} X_f L_f \left[\frac{\sqrt{V(\text{gpm}/\text{ft}^2)}}{1 + 0.0443(L_f - 30)} \right]^{0.58} \quad \text{when } L_f > 30 \text{ } \mu\text{m} \quad (17)$$

$$= 2.90 \times 10^{-7} X_f L_f V^{0.29} \quad \text{when } L_f < 30 \text{ } \mu\text{m} \quad (18)$$

Figure 5 shows a plot of the Biomass Slough-off rate versus the liquid flow rate per unit cross-sectional area of the biofilter. As the liquid loading increases, the biomass slough-off rate also increases, but the rate of increase decreases at higher loadings. Also, included in this figure are inlet contaminant concentrations when the biomass generation rate is balanced by the biomass slough-off rate. Physical slough-off of the biomass is the only effective strategy to maintain biomass holdup within the biofilter and prevent accumulation of excess biomass, which eventually results in excessive gas-phase pressure drop through the biofilter bed. However, physical slough-off of the biomass from the media does not imply that the biomass has been removed. The design of the media has to allow this physical removal of this sloughed-off biomass from the bed, which otherwise would result in accumulation and clogging.

Table 4 gives the model equations for a synthetic media biofilter, which includes the effects of mass transfer and biokinetics. From equation (4.8) the fractional efficiency of a synthetic media biofilter can be approximated by the following equation:

$$E \approx \frac{A_s D_{Biofilm} X_f \tau k}{u_g C_g^i \varepsilon} \quad (19)$$

Using the following definitions for Loading and Elimination Capacity:

$$\text{Loading (g / m}^3 \cdot \text{h)} = \frac{QC_g^i}{V_{Bed}} = \frac{C_g^i}{\tau} \quad (20)$$

$$\text{Elimination Capacity (g/m}^3 \cdot \text{h)} = \frac{QC_g^i (1-E)}{V_{Bed}} = \frac{C_g^i (1-E)}{\tau} \quad (21)$$

Combining equations (19), (20) and (21), we get

$$\text{Elimination Capacity} = \text{Loading} - \frac{A_s D_{\text{Biofilm}} X_f k}{u_g \varepsilon} \quad (22)$$

When the Biofilter operates at 100% Removal Efficiency, i.e., $E = 1$, the Elimination Capacity = Loading, and hence:

$$E = 1.0 = \frac{A_s D_{\text{Biofilm}} X_f \tau k}{u_g C_g^i \varepsilon} \quad (23)$$

Using the definition of Maximum Elimination Capacity when $E = 1$ and equation (23) we get:

$$EC_{\text{Max}} = \left(\frac{C_g^i}{\tau} \right)_{E=1} = \left(\frac{A_s}{\varepsilon} \right) \left(\frac{D_{\text{Biofilm}} k X_f}{u_g} \right) \quad (24)$$

The maximum elimination capacity (EC_{Max}) has been written as a product of two factors: (1) Biofilter Elimination Capacity Media factor = $B_{EC} = (A_s/\varepsilon)$; and (2) Biokinetics factor = $(D_{\text{Biofilm}} k X_f / u_g)$. For this maximum elimination capacity to be as high as possible, the biofilter synthetic media should have the highest possible value of the Media Elimination Capacity Factor.

Another important consideration in biofiltration is gas-phase pressure drop. As mentioned earlier, gas-phase pressure drop depends on the ability of the media to allow sloughed-off biomass to exit the bed. It also depends on the thickness of biofilms, bed void fraction, packing media characteristics and gas flow rate. Since the gas-phase residence time in the biofilter bed, τ , can be written as H/u_g , equation (23) becomes:

$$\left(\frac{A_s}{\varepsilon} \right) \left(\frac{D_{\text{Biofilm}} k X_f}{1} \right) \left(\frac{H}{C_g^i u_g^2} \right) = 1 \quad (25)$$

The gas-phase pressure drop in the bed per unit height of biomedica can be written as follows (Treybal, 1980):

$$\frac{\Delta P}{H} = C_D \rho_g u_g^2 \quad (26)$$

where ΔP is the gas-phase pressure drop through the biomedica bed of height H , and C_D is an empirical friction factor for the specific type of biomedica packed bed. Combining equations (25) and (26), for 100% removal efficiency, we get:

$$\Delta P = \left(\frac{A_s C_D}{\varepsilon} \right) \left(\frac{D_{\text{Biofilm}} k X_f \rho_g}{1} \right) \left(\frac{H^2}{C_g^i} \right) \quad (27)$$

For minimum gas-phase pressure drop, the following biomedica pressure drop factor should be maximum:

$$\text{Biomedica Pressure Drop Factor} = B_{\Delta P} = \left(\frac{\varepsilon}{A_s C_D} \right) \quad (28)$$

Considering both the objectives of maximum elimination capacity and minimum gas-phase pressure drop, both the biomedial factors, B_{EC} and B_{AP} , must be maximized for a specific size of biomedial. Figure 6 shows a plot of these two biomedial factors for ceramic Raschig Rings, using data on bed void fraction, specific area of packing per unit volume of packed bed and empirical friction factor (Treybal, 1980), ignoring the effect of liquid holdup in the bed, presence of biofilm, etc. Clearly, there exists an “optimum” biomedial nominal size that will maximize the elimination capacity and pressure drop factors.

Ideal characteristics of synthetic media are as follows: (1) high specific surface area, which is the area of the biofilm exposed to the gas-phase contaminants. Most synthetic media have specific areas between $30 \text{ ft}^2/\text{ft}^3$ ($100 \text{ m}^2/\text{m}^3$) to $300 \text{ ft}^2/\text{ft}^3$ ($980 \text{ m}^2/\text{m}^3$); (2) High void fraction, which is the percentage of open space in the packing. Void fractions generally have to be higher than 90% to be effective as a biofilter media; (3) Large free passage diameter, which is the diameter of the largest sphere that will pass through the packed media. Large free passage diameter is necessary to allow excess biomass to not only slough-off the surface but also exit the bed, so that biomass accumulation does not result in media clogging and channeling; (4) Rigid material which does not compact with biomass growth. Fibrous mats and foam generally begins to compact down due to biomass growth, resulting in lower void fractions and eventually high gas-phase pressure drop; (5) Provide good biofilm attachment on its surface. Generally surface roughness, charge and hydrophobicity are important variables that need to be optimized for effective biofilm attachment; (6) Low gas-phase pressure drop. The operating cost of the biofilter system depends mainly on the gas-phase pressure drop, which generally has to be less than 5 inches of water column, to be cost effective; and (7) Low media cost per unit volume. Since biofilters are used to treat a wide range of gas flow rates, as high as 150,000 cubic feet per minute, and empty-bed gas-phase residence times have to be less than 10 minutes for manageable vessel costs, the volume of media required can be very large and hence cost of media can be a critical factor in achieving acceptable biofiltration total costs per cubic feet of gas treated.

5. Randomly Packed versus Structured Biomedial

Structured packing consists of regular elements which are combined together to form an insert block. Usually, these insert blocks can be made of any size and are manufactured from thin-walled materials, which reduces bulk density of the media. Structured packing exhibits a higher surface area per unit volume than random packing, in which the packing element are randomly packed in the bed. Since, structured packing offers parallel flow arrangement, it exhibits lower gas-phase pressure drop and can handle higher biomass growth than random packings. Hence, structured packings are more suited for handling streams containing high Biological Oxygen Demand (BOD), which result in increased biomass growth. Also, structured packings are easier to clean using the shear force of the liquid flow, than random

packing, which offer a tortuous path through the bed, and which usually result in holding the biomass within the bed, even after it is sloughed-off the media surface. This makes structured packings more suitable when biomass clogging can occur due to increased biomass growth or presence of solids in the gas or liquid stream.

Random packings consist of many shapes and sizes, ranging from simple Raschig Rings to other shapes, such as Berl saddles, fibers, open-cell foams, porous ceramic cylinders, lava rock pieces, etc. Most of these media were developed for gas absorption towers, where it was desired to create a thin liquid film on the media surface to maximize the gas absorption of the contaminant from the gas to liquid phase. However, in the case of biofilters, growth of biofilm on the surface of the media is of paramount importance for efficient operation of the biofilter system. Since attached biofilms retain water within their structure, the emphases in biofilter systems is to keep these biofilms moist and prevent them from drying, rather than in creating a liquid film on the biofilm surface. Usually, if a liquid film is created on the biofilm, it would present additional resistance for mass transfer, especially if the contaminant(s) being treated have low water solubility.

While surface area, bulk density, cost are important parameters in the selection of randomly packed biomedias, the most important characteristics for short start-up time in biofiltration was found to be water retention capacity. Water retention capacity, defined as volume of water held within the packing media per unit volume of packed media, consists of two terms: (1) static liquid holdup, which is a function of packing media design and packing factor; and (2) dynamic liquid holdup, which varies with gas velocity and pressure drop, especially in counter-current flow. Since dynamic liquid holdup changes with direction of gas and liquid flows and gas flow rates, static liquid holdup was used as an important parameter in evaluating randomly packed media for biofiltration applications.

Static holdup occurs as a result of two factors:

1. Design of the packing, leading to interstitial holdup at the points of contact between the various units of the packing media and contact points of the surfaces within the unit packing structure; and
2. Adhesion of the liquid to the media's surface, especially during startup, when the biofilm has just begun to nucleate and grow.

Static holdup in packed beds is related to Residual Saturation, which is defined as the volume of liquid holdup after the packed bed is allowed to drain completely by gravity. Previous work has shown that a dimensionless quantity, Capillary Number, effectively expresses the ratio of the water draining driving force (gravity) and the liquid retention forces in the bed. The Residual Saturation, S_R , is defined as follows:

$$S_R = \frac{\text{Residual Holdup of liquid in bed}}{\text{Bed Void Volume}} \quad (29)$$

The Capillary Number, defined by using the Carman-Kozeny equation, can be written as follows (Wakeman, 1979):

$$Ca = \frac{\varepsilon^3 d_s^2 \rho_f g}{(1 - \varepsilon)^2 \sigma \cos \theta} \quad (30)$$

where ε = bed voidage; d_s is the equivalent diameter of a sphere with the same surface area as a single packing media element; ρ_f is fluid density; σ is surface tension of water; and θ is the contact angle, which in the case of biofilter would be 0. A correlation has been developed between the Residual Saturation and the Capillary Number using data from packed beds and consolidated sands (Swindells, 1982):

$$S_R = \frac{Ca^{-0.27}}{15.6} \quad (31)$$

Figure 7 shows a plot of the Residual Saturation and the Static Holdup for two different types of media used in gas absorption towers (Treybal 1980). The Residual Saturation correlates strongly with the Static Holdup, and these two parameters represent the potential of the packing media to allow initial biomass growth, since it allows water to remain in the column for a longer period of time and produces higher mass transfer coefficients due to higher tortuosity of the gas flow path through the packing media.. As the size of the packing media decreases, the Residual Saturation increases. However, as the media size decrease, the potential for clogging of the media due to biomass growth also increases. Hence, biofilter media has to be designed to offer high Residual Saturation with large openings for excess biomass to be removed from the bed. Structured media have very low Residual Saturation, and hence are not suitable as biofilter media, even though they exhibit low gas-phase pressure drop, and very high surface areas. The only exception is when the structured media are composed from porous media walls, which exhibit water retention capacity, as in the case of ceramic monoliths used in the experimental studies, presented in this chapter. In addition, these monoliths have very low gas-phase pressure drop, exhibit high specific surface areas per unit volume of bed, and excess biomass can be easily sloughed-off the walls and can exit the bed due to its straight open passages. However, a major disadvantage of ceramic monoliths is their high cost.

6. Biofilter versus Biotrickling Filter

In the literature, the term “biofilter” has been used to describe systems which traditionally have used naturally bioactive media, with water retention capacity, which has required the use of humidified air and periodic water addition, rather than a continuous flow of aqueous nutrients. Naturally bioactive media has bioavailable nutrients (nitrogen and phosphorus trace minerals, etc.) for biodegradation, and hence do not require continuous addition of nutrients. The term “biotrickling filter” is used for systems which have a continuous flow of aqueous nutrients flowing through a bed of synthetic media. A continuous flow of liquid is needed since the media usually has low Residual Saturation and none or low water retention capability. In addition, continuous flow of water allows excess biomass to be sloughed-off, provide the nitrogen and phosphorus nutrients needed for biodegradation, and buffer any pH changes which might occur due to production of either acidic or basic by-products, such as sulfate, hydroxide, nitrate, etc. In the case of naturally bioactive media, continuous water flow will result in segregation of smaller particles in the bottom section of the bed due to hydraulic transport, which would result in clogging of media and increase in gas-phase pressure drop.

The only difference between a biofilter and a biotrickling filter is that in a biofilter the media has sufficient water holding capacity to maintain bioactivity using humidified air, while in a biotrickling filter, a continuous flow of water is necessary to maintain moisture content in the active biofilms, since the Residual Saturation or Water Holdup in the media is insufficient, especially since larger media size has to be used to minimize the potential for clogging, which reduces the water holdup in the media, as shown in Figure 7.

7. Experimental Studies on Diffusive Biofilter Media

The objective of this study is to test the effect of support media on biofilter performance. Isopentane was chosen as the target in this study, since it is used as a blowing agent in the manufacture of foam products.

7.1 Experimental Set-up

A schematic of the experimental system is shown in Figure 8. Series of glass biofilters systems were assembled to test different support media. Each glass biofilter was made in two sections with the total height of 90 cm and diameter of 5 cm. It had provisions of six side ports for withdrawing gaseous samples. Another small glass biofilter was built to carry out the temperature and water content effect tests. This small biofilter was 2.5 cm in diameter and had total volume of 100 ml. It had a water jacket outside to control temperature using a water bath. Compressed air was delivered to the bottom of the biofilter

after passing through a counter-current packed pre-humidifier column. The gas flow rate was controlled by a thermal mass flow controller (MKS Industries, Type 1259, Control channel type 247). The desired concentration of the iso-pentane in the air stream was obtained by injecting the pure chemical into the air stream using a syringe pump. Nutrient solution (Govind and Bishop 1998) was pumped from the nutrient reservoir bottle to the top of the biofilter. The contaminated air stream flowed counter-currently to the trickling nutrient solution.

Biomass from a pilot scale activated sludge plant treating hazardous waste was suspended in an aerated aqueous phase bioreactor (column 100 mm diameter, 700 mm height). The bioreactor was fed daily with iso-pentane. Nutrients were also added periodically. The acclimated biomass from the bioreactor was later used to seed the synthetic support media.

Five different support media were tested in this study. Peat and compost were chosen as the naturally bioactive media with effective particle diameters of 3.5 mm and 2.5 mm respectively. The water content of peat was 0.645 g water/g dry peat. The compost water content was 0.536 g water/g dry compost. Celite pellets (Manville Corp., Denver, CO), with a diameter of 6 mm were packed into the biofilter. Cordierite monolith, with and without a coating of activated carbon, obtained through Dow Corning, Corning, NY, with 50 square channels per square inch (channel dimension of 2 mm x 2mm), were used as structured media. The biofilters were operated continuously an inlet and outlet composition data were collected over a period of time. The concentration profiles of the compounds in the biofilter were obtained by withdrawing samples from the side ports and analyzing them using gas chromatography. Once the biofilter performance reached steady state, the concentration difference of carbon dioxide in the gas phase were measured to assess the mineralization of all compounds.

7.2 Analytical Procedure

The gas samples taken from the sampling ports were analyzed by gas chromatography in Tracor 585 gas chromatography fitted with DB-624 column (60 cm long, 0.53 mm diameter) using photoionization and electrolytic conductivity detectors. Helium was used as the carrier gas. pH of the solutions was measured by combination pH electrode. Carbon dioxide concentration in gas streams was determined in a Fisher 1200 gas partitioner.

7.3 Results and Discussion

7.3.1 Adsorption Capacity

400 ml fresh samples of support were take for each media. The contaminated gas was introduced at the flowrate of 100 ml/min with the inlet concentration of 350 ppmv. The break through curves of all five support media are shown in Figure 9. It was found that the natural support media like peat and compost had limited adsorption capacity. The celite pellets and cordierite monolith systems had low

adsorption capacity while the activated carbon coated monolith system exhibited higher adsorption capacity.

7.3.2 Water Content Effect

The removal efficiency of iso-pentane in peat and compost biofilters, using different media water content, were tested in the small glass biofilter. The contaminated gas was introduced at 20 ml/min with an inlet concentration of 470 ppmv. Figure 10 shows the effect of water content on the operating efficiency of a peat and compost packed-bed. The removal efficiency was maximized when the water content was in the range of 0.62 - 0.67 g water /g dry media. When the water content was less than 0.57 g water /g dry peat and 0.58 g water/g dry compost, an irreversible loss of biofilter efficiency occurred, as shown by the dotted line. Above a water content of 0.67 g water /g dry media, there was a significant decrease in operating efficiency, mainly due to the blanketing of the material macropores by free water, coupled with low aqueous solubility of iso-pentane.

These results show the importance of maintaining water content within a narrow range in biofilters using these kinds of naturally bioactive media. There was an “optimum” water content, below and above which, the biofilter removal efficiency declined. Typically shallow beds with large cross-sectional areas and inlet air humidification are used to effectively maintain water content in the media during operation.

7.3.3 Temperature Effect

As temperature increased in the 25°C to 40°C range, increased biodegradation rates were observed, which is typical for biochemical reactions. The data was used to obtain the activation energy for net growth of biomass in naturally bioactive systems, and this value was in the range of 1.9 – 2.4 kJ/mole.

7.3.4 Steady State Operation

Biofilters with different support media were operated under various operating conditions. Carbon dioxide measurements of the inlet and outlet gases were used to confirm these removal efficiencies. The removal efficiency increased at lower inlet iso-pentane concentrations and at higher gas retention times. Celite pellets and cordierite monolith showed similar performance at steady state since they had similar surface area for biofilm growth. The carbon-coated monolith biofilter showed 10 ~ 20% higher removal efficiency and this was attributed to iso-pentane adsorption and subsequent desorption into the biofilm, which resulted in thicker biofilms. Synthetic media biofilters exhibited higher removal efficiencies than naturally bioactive media, peat and compost, and Figure 11 shows a comparison of the different media, based on iso-pentane biotreatment rates.

8. Experimental Studies on Convective Biofilter Media

Two identical biofilters were constructed using ceramic monoliths, each with dimension of 13 cm width x 15 cm length x 9 cm height. Each ceramic monolith were coated with a thin layer of activated carbon, and there were 10 square cells per square inch, with each cell being 0.45 cm x 0.45 cm dimension. The porous walls between each cell had a thickness of 0.2 mm and an average pore size of 30 μm . In these monoliths, contaminated air would enter one end of the monolith and flow out through the other end, as shown in Figure 12a. In this case, the contaminant in the gas phase would diffuse to the porous walls of the monolith, perpendicular to the direction of gas flow, and this would be diffusive type of biofilter media. In the second monolith, alternate channels were plugged at the outlet end, as shown in Figure 12b, which would force the contaminated gas to flow into the open channels and then flow through the biofilm and porous walls of the cells to exit through the channels that were open at the exit end of the monolith. In this case, there would be convective flow of contaminant through the biofilm, instead of diffusive, and this type of media would be classified as convective type of biofilter media, as discussed earlier in this chapter. Both monoliths were identical except in the direction of flow of the contaminant into the biofilms, and both monoliths were operated under identical flow and contaminant concentration conditions.

Contaminants studied were ethanol and toluene. Both contaminants were analyzed using HP 5710 gas chromatograph, equipped with a flame ionization detector (FID) and an Alltech 10% CBWX 20 M CWHP 80/100, 6' x 1/8" stainless-steel packed column (Stock No. 12106PC, Serial No. 1082-21753). The oven temperature was set at 60°C, injector temperature at 150°C, and detector temperature at 300°C, with nitrogen as the carrier gas. Analysis of carbon dioxide was performed using HP 5890 Series II gas chromatograph equipped with a thermal conductivity detector using a 6 feet Porapak 80/100 mesh packed column, with oven temperature at 110°C and a run time of 5 minutes.

Figure 13 shows the toluene elimination capacity versus the loading for the convective and diffusive modes of operation. Clearly, the convective flow shows a higher elimination capacity than the diffusive, and this difference in performance has also been shown using a mathematical model (model lines are shown in Figure 13; Fang and Govind 2002).

9. Studies on Encapsulated Biomass and Membrane Biofilters

Gel entrapment of active bacterial cultures was achieved using a modified procedure originally used by Fukushima et al. (1988). Colloidal silica SM grade (30% silica, 7 nm average particle size, 1.22 specific gravity) was pH adjusted to 7.0 using 5N HCl and the solution was maintained at room temperature with gentle stirring. 2 gm of agarose (gelling temperature of 28°C and melting point of 65°C) is mixed with 50 mL of water at room temperature, and then heated above melting point with gentle stirring. 1% low viscosity alginate is separately dissolved in 50 mL water and mixed to obtain a clear solution. Centrifuged biomass is added to the alginate solution, and the resulting sol and biomass mixture is added to the agarose sol at 35°C to completely disperse the biomass in the combined sol mixture. Just before gel pellets are synthesized, the combined alginate-biomass sol is added to the silica sol and the resulting solution is dropped into 5% calcium chloride solution to form beads with an average diameter of 3 mm. The bacterial cells are now entrapped in the gel matrix inside the beads, and are active and capable of degrading contaminants.

The experimental system mainly consisted of a 2 inch diameter (5 cm) glass column, packed with 10 cm height of 3 mm diameter gel beads. The reactor had a liquid sump of about 100 mL and a headspace of 500 mL. Both the liquid and gas phases were recycled in a batch mode (liquid flow rate of 10 mL/minute and gas flow rate of 30 mL/minute) and the contaminant concentration in the gas phase was analyzed using gas chromatography. Figure 14 shows the degradation of toluene, which demonstrated the existence of active biomass encapsulated within the pellets. Figure 15 shows the degradation of perchloroethylene (PCE) with sodium acetate present in the liquid sump. While complete details of these results have not been provided here for the sake of brevity, corresponding measurements of gas-phase carbon dioxide and chloride ion in the liquid phase verified the biological breakdown of the perchloroethylene. The mechanism of PCE degradation is shown in Figure 16, in which PCE diffuses into the anoxic zone within the gel bead and dechlorinates into less chlorinated by-products, which degrade into carbon dioxide and water in the outer region of the bead due to the diffusion of oxygen from the outer surface of the bead. The inner anoxic zone is surrounded by an aerobic zone, and these two zones with widely different oxidation-reduction potentials co-exist within the same gel bead. The bead accomplishes the breakdown of PCE through a synchronous anaerobic-aerobic degradation process, and detailed analysis of this mechanism has been presented elsewhere (Tabak et al. 2001).

Membranes offer high surface areas on which biofilms can be attached. In membrane biofilters, usually hollow fibers are used to develop biofilms outside the porous surfaces, by flooding the shell side with nutrients. Contaminated air flows on the inside of the porous hollow fibers, with the contaminant diffusing into the active biofilms through the pores. Membrane biofilters have been used to successfully

biodegrade toluene, trichloroethylene (TCE) (Parvatiyar et al. 1996a; 1996b). Major problems encountered with membranes are pore plugging due to slime produced by aerobic organisms and additional mass transfer resistance due to the membrane itself. However, they offer a compact design, with very high contact surface areas for biofiltration applications.

10. Conclusions

Media characteristics are of critical importance in the effective operation of any biofilter system. Broadly, biofiltration media can be classified as either being inherently bioactive (naturally bioactive media) or synthetic, which has to be initially inoculated to achieve biomass growth. Naturally bioactive media are suitable for odor biofiltration, where the contaminant loading is low. At high contaminant loadings, as in biofiltration treatment of volatile organic emissions, synthetic media biofiltering filters are generally more effective. There are a wide variety of synthetic media, and in terms of their mass transfer characteristics, can be classified as being either diffusive or convective. Very few studies on convective biofiltration have been conducted. Diffusive biofiltration becomes inefficient either when the biofilms are thick and/or when the bulk contaminant concentration is low, as usually in odor biofiltration.

Adsorption of the contaminants on the media's surface offers an additional mechanism for biodegradation, namely backdiffusion of the adsorbed contaminant into the biofilm, and eliminates the concept of maximum biofilm thickness, as in the case of non-adsorptive media.

There is an "optimum" synthetic media nominal size which maximizes the biotreatment efficiency and minimizes the gas-phase pressure drop. The residual saturation reflects the capacity of the media to hold water, and affects the start-up time of the biofilter system. Several experimental studies have been conducted to obtain a better understanding of the role of biofilter media, and some of these results were presented in this chapter.

Encapsulated biomass biofilters offer a new type of biofilter media, which can create synchronous aerobic-anoxic zones, especially for breakdown of chlorinated compounds, such as perchloroethylene (PCE), which are otherwise aerobically recalcitrant.

Membrane biofilters offer advantages of compact sizes, high surface areas, and effective contact between the contaminated gas and biofilms. However, they generally suffer from clogging of membrane pores due to slime, usually generated by aerobic organisms. More research work is needed on these systems to effectively use them for industrial and municipal biofilter applications.

11. References

- Accardi-Dey A, Gschwend PM (2002) Assessing the combined roles of natural organic matter and black carbon as sorbents in sediments *Environ Sci Technol* 36: 21-29
- Bendinger B, Rijnaarts HHM, Altendorf K, Zehnder AJB. (1993) Physicochemical cell surface and adhesive properties of coryneform bacteria related to the presence and chain length of mycolic acids. *Appl Environ Microbiol* 59: 3973-3977.
- Characklis WG, McFeters GA, Marshall KC (1990) Physiological ecology in biofilm systems. In: Characklis WG, Marshall KC (eds) *Biofilms*. John Wiley & Sons, New York, pp 341-394.
- Charpentier JC (1976) Recent progress in two-phase gas-liquid mass transfer in packed beds *Chem Eng* 11: 161-167.
- Chiou CT, Kile DE, Rutherford DW, Sheng G, Boyd SA (2000) Sorption of selected organic compounds from water to a peat soil and its humic-acid and humin fractions: potential sources of the sorption nonlinearity *Environ Sci Technol* 34: 1254: 1258.
- Chiou CT, Porter PE, Schmedding DW (1983) Partition equilibria of nonionic organic compounds between soil organic matter and water. *Environ Sci Technol* 17:227-231
- Cowan MM, Warren TM, Fletcher M (1991) Mixed species colonization of solid surfaces in laboratory biofilms. *Biofouling* 3:23-34.
- Dubinin MM, Astakhov VA (1971) Development of concepts of volume filling of micropores in adsorption of gases and vapors by microporous adsorbents. *Izv Akad Nauk SSSR, Ser Khim* 1: 5-11.
- Fang J, Govind R (2002) Unpublished data.
- Fletcher M (1988) The applications of interference reflection microscopy to the study of bacterial adhesion to solid surfaces. In: Houghton DR, Smith RN, Eggins HOW (eds) *Biodeterioration 7*. Elsevier Applied Science, London, pp 31-35.
- Fletcher M (1988) Attachment of *Pseudomonas fluorescens* to glass and influence of electrolytes on bacterium-substratum separation distance. *J Bacteriol* 170: 2027-2030.
- Fletcher M, Loeb GI (1979) Influence of substratum characteristics on the attachment of a marine pseudomonad to solid surfaces. *Appl Environ Microbiol* 37: 67-72.
- Fukushima Y, Okamura K, Imai K, Motai H (1988) A new immobilization technique of whole cells and enzymes with colloidal silica and alginate. *Biotech Bioengng* 32: 584-594.
- Gao C., Govind R., Tabak H. (1996) Predicting soil sorption coefficients of organic chemicals using neural network model. *Env Tox and Chem* 15: 1089-1096.
- Govind R (2002) Biofiltration: New Technology for the metal finishing industries. *Finishers Management* 4: 56-62.

- Govind R, Bishop DF (1998) Biofiltration for treatment of volatile organic compounds (VOCs) in air. In: Sikdar SS, Irvive RI (eds) Biodegradation Technology Developments, Volume II. Technomic Publishing Company, Lancaster, PA, USA, pp 403-460.
- Karickhoff SW, Brown DS, Scott TA (1979) Sorption of hydrophobic pollutants on natural sediments. *Water Res* 13:241-248
- Loeb GI, Neihof RA (1975) Marine conditioning films. *Advances in Chemistry* 145: 319-335.
- Parvatiyar MG, Govind R, Bishop DF (1996a) Biodegradation of toluene in a membrane biofilter. *J Mem Sci* 119: 17-24.
- Parvatiyar MG, Govind R, Bishop DF (1996b) Treatment of trichloroethylene (TCE) in a membrane biofilter *Biotech Bioengng* 50: 57-64.
- Polanyi M. (1916) Adsorption von Gasen (Dampfen) durch ein festes nichtfluchtiges Adsorbens. *Berichte Deutsche Physikalische Gesellschaft* 18: 55-80.
- Pringle JH, Fletcher M. (1983) Influence of substratum wettability on attachment of freshwater bacteria to solid surfaces. *Appl Environ Microbiol* 45: 811-817.
- Ramani M, Govind R (2002) Unpublished data.
- Rittmann BE (1989) Detachment from biofilms. In: Characklis WG, Wilderer PA (eds) *Structure and function of Biofilms*. The Bath Press Ltd, Bath, Avon, England, pp 49-58.
- Rosenberg M, Kjelleberg S (1986) Hydrophobic interactions in bacterial adhesion. *Advances in microbial ecology* 9: 353-393.
- Seth R, Mackay D, Muncke J (1999) Estimating the organic carbon partition coefficient and its variability for hydrophobic hemicals *Environ Sci Technol* 33: 2390-2394.
- Swindells RJ (1982) A mathematical model of a continuous sugar centrifuge. PhD thesis, University of Queensland, Australia.
- Tabak HH, Govind R, Ramani M (2001) In-situ bioremediation of contaminated sediments using membranes and gel beads. In: Leeson A, Foote E, Banks K, Magar, VS (eds) *Phytoremediation, Wetlands, and Sediments*. Battelle Press, Columbus, OH, USA, pp 200-210.
- Treybal (1980) *Mass transfer operations*. McGraw-Hill Company, New York.
- Wakeman RJ, Rushton A, Brewis LN (1976) Residual Saturation of dewatered filter cakes. *The Chemical Engineer* 314: 668-670.
- Weber Jr WJ, Huang W, LeBoeuf EJ (1999) Geosorbent organic matter and its relationship to the binding and sequestration of organic contaminants. *Colloid Surf A: Physicochem Eng Aspect* 151: 167-179.
- Xia G. (1998) Sorption behavior of nonpolar organic chemicals on natural sorbents. PhD Thesis, The John Hopkins University, Baltimore, MD.

Xing G, Pignatello JJ (2001) Detailed sorption isotherms of polar and apolar compounds in a high organic soil. *Environ Sci Technol* 35:84-94.

Zhao W, Govind R (1997) Biofiltration of iso-pentane in peat and compost packed-beds. *AIChE J* 43: 1348-1356.

FIGURES LEGENDS

Figure 1. Schematic of Diffusive and Convective Support Media in Biofiltration: (a) Non-adsorptive Diffusive ; (b) Adsorptive Diffusive, with back-diffusion of contaminant from the media's surface into the biofilm; and (c) Convective, with gas flow through the biofilm and porous support media.

Figure 2. Biomedia surface with attached biofilm.

Figure 3. Plot of Biofilm Effectiveness Factor versus the Normalized contaminant concentration, and as a function of Thiele's Modulus ($\sqrt{\alpha}$).

Figure 4. Effect of Water Content on Biofilter Removal Efficiency.

Figure 5. Biomass Slough-off Rate versus the Liquid Flow Rate in the Biofilter.

Figure 6. Plot of Maximum Elimination Capacity and Minimum Pressure Drop Biomedia Factors versus the Nominal Size.

Figure 7. Residual Bed Saturation and Static Water Holdup in the Biofilter Bed for two different kinds of Packings.

Figure 8. Schematic of the experimental system for studying different kinds of Biomedia.

Figure 9. Iso-pentane outlet concentration as a function of gas-phase residence time (empty bed) for different biomedia.

Figure 10. Effect of water content on removal efficiency of iso-pentane in peat and compost biofilters.

Figure 11. Comparison of different biomedia in terms of the maximum elimination capacity for iso-pentane.

Figure 12. Monolith support media used in biofilter: (a) Diffusive, with gas entering and exiting through the straight passages; and (b) Convective, with gas entering and then flowing through the biofilms and porous walls of the monolith, by alternate blocking of passages in the top and bottom surfaces of the media.

Figure 13. Removal Capacity of Toluene in a Diffusive and Convective Monolith Support Media Biofilter as a function of inlet concentration. The straight lines are model fits.

Figure 14. Exit concentration of toluene as a function of time in a silica gel bead encapsulated biomass biofilter, operated in batch mode.

Figure 15. Concentration of acetate (liquid phase) and perchloroethylene (PCE) in the gas phase of a silica gel bead encapsulated biomass biofilter, operated in batch mode.

Figure 16. Schematic showing the mechanism of PCE degradation within the anoxic and aerobic zones that simultaneously co-exist within the gel bead.

Table 1. Model Equations for a Naturally Bioactive Media Biofilter.

Equation Number	Model Equation	Explanation
1.1	$\left(\frac{D_e}{r^2}\right)\frac{\partial}{\partial r}\left[r^2\frac{\partial C}{\partial r}\right] = R_B \quad 0 \leq r \leq R$	Diffusion and reaction within the porous compost particle of radius R
1.2	$R_B = \frac{KC}{K_C + C} \frac{(W - W_i)}{K_{CW} + (W - W_i)} \quad W_i < W < W_p$	Rate of biodegradation of contaminant in the porous compost particle, which accounts for water content
1.3	$r = 0 \quad \frac{dC}{dr} = 0$ $r = R; \quad D_e \left. \frac{\partial C}{\partial r} \right _{r=R} = k_g (C_b - C_f)$	Boundary conditions. Symmetry condition at the center of the particle, and mass transfer balance at the outer boundary of the particle
1.4	$\frac{k_g P}{\rho_g u_g} = 2.3 \frac{(aR)^{-1.7}}{MW_s} \left(\frac{u_g \rho_g R}{\mu_g}\right)^{-0.3} \left(\frac{\mu_g}{\rho_g D_g}\right)^{-0.5}$	Gas-phase mass transfer coefficient for packed beds (Charpentier 1976)
1.5	$k_l = \frac{3D_l(1+W_o)(1-\varepsilon)}{\rho_l R(W - W_p)} \quad W_p < W < W_{\max}$	Mass transfer coefficient in the liquid phase film outside the compost particle
1.6	$r = 0 \quad \frac{dC}{dr} = 0$ $r = R; \quad D_e \left. \frac{\partial C}{\partial r} \right _{r=R} = K_g (C_b - C_f)$	Boundary conditions for the case of water film outside the compost particle. Symmetry condition at the center of the particle and mass transfer balance at the surface
1.7	$\frac{1}{K_g} = \frac{1}{k_g} + \frac{1}{HNk_l}$	Overall mass transfer coefficient as a function of the gas and liquid mass transfer coefficients
1.8	$u_g \left(\frac{\partial C}{\partial Z}\right) + 3 \left[(1-\varepsilon) \frac{D_e}{R} \right] \left(\frac{\partial C}{\partial r}\right)_{r=R} = 0$	Mass balance of contaminant along the biofilter height
1.9	$Z = 0 \quad C = C_{in}$	Boundary condition at biofilter inlet
1.10	$\left(\frac{D_{eo}}{r^2}\right)\frac{\partial}{\partial r}\left[r^2\frac{\partial C_o}{\partial r}\right] = R_{Bo} \quad 0 \leq r \leq R$	Oxygen diffusion and utilization inside the compost particle due to aerobic biodegradation of contaminant
1.11	$R_{Bo} = \beta R_B$	Stoichiometric balance between the rates of oxygen consumption and contaminant biodegradation

Table 2. Advantages and Disadvantages of using Naturally Bioactive Media in Biofilters.

Advantages	Disadvantages
<ol style="list-style-type: none"> 1. Low cost 2. Inherent bioactivity within media 3. Physical adsorption of contaminant 4. Chemical complexation of some organic contaminants 5. Mimics natural ecosystem 	<ol style="list-style-type: none"> 1. Settling of media due to biomass growth 2. Cannot separate biomass growth from the media 3. Eventual consumption of bioavailable nitrogen and phosphorus, requiring media replacement 4. Water content has to be maintained to prevent drying or excess water in the media 5. Low biodegradation rates, requiring large volume of media 6. Limited bed height results in large cross-sectional area 7. Large bed sizes increases cost of vessel 8. Significant gas-phase pressure drop 9. Inability to effectively neutralize acidic by-products 10. Possible oxygen transfer limitations at high contaminant loadings 11. Possible channeling of gas through the bed 12. Significant bulk density of media

Table 3. Advantages and Disadvantages of various types of synthetic* biofilter media.

Packing Configuration	Type of Synthetic Media	Advantages	Disadvantages
Randomly Packed	Granular (gravel, lava rock, wood chips etc)	<ul style="list-style-type: none"> - Low cost and easily available - Rough surface for biofilm attachment - Has been used in old trickling filters (water treatment) - Has metal content which can react with hydrogen sulfide to form metal sulfides 	<ul style="list-style-type: none"> - Low surface area - Low void fraction – can be easily plugged - High bulk density (heavy weight) - Gas channeling - High gas pressure drop, if small size
	Fibrous mesh pads	<ul style="list-style-type: none"> - High surface area - Low bulk density - Low gas-phase pressure drop - Biofilm surface area increases with biofilm thickness 	<ul style="list-style-type: none"> - Small free passage diameter; hence can be easily clogged - Compacts due to weight of biomass growth, increasing pressure drop and causing clogging - Does not distribute trickling water evenly
	Open cell polymeric foam	<ul style="list-style-type: none"> - Good retention of water - High surface area - Low bulk density - Retains biomass growth - High porosity 	<ul style="list-style-type: none"> - Depending on number of pores per inch, can be easily clogged - Difficult to slough-off biomass growth - Compacts due to biomass weight - Does not distribute trickling water evenly
	Extruded plastic packing (Raschig rings, Berl saddles, etc.)	<ul style="list-style-type: none"> - Commercially available in many sizes and shapes - Good liquid distribution - Low gas pressure drop - Low bulk density - Some designs have high void fraction - Good gas-liquid contact 	<ul style="list-style-type: none"> - Developed for gas absorption towers, where the liquid flow rates are much higher - Surface unsuitable for biofilm attachment and growth - Insufficient void fraction, especially with small sizes
Structured	Extruded Plastic	<ul style="list-style-type: none"> - High surface area - Low gas-phase pressure drop - High void fraction - Low bulk density - Large free passage diameter - Easily supported 	<ul style="list-style-type: none"> - Plastic surface unsuitable for biofilm attachment and growth - Originally developed for trickling filter (water treatment) - Have to be cut to fit vessel - High cost per unit volume
	Ceramic	<ul style="list-style-type: none"> - High surface area - Low gas-phase pressure drop - High void fraction - Low bulk density - Large free passage diameter - Easily supported - Can be used as convective media 	<ul style="list-style-type: none"> - Have to be cut to fit vessel - High cost per unit volume - Not manufactured in large sizes - Few experimental studies in biofiltration

* “synthetic” here means either manufactured or cut from natural materials without any inherent bioactivity

Table 4. Model Equations for a Synthetic Media Biofilter.

Equation Number	Equation	Explanation
4.1	$J _{x=x_{AB}} = \frac{-D_{Biofilm}}{(u_g + b)} R_B$	Flux of contaminant at the Air (A) and Biofilm (B) interface
4.2	$R_B = \frac{kX_f C_s}{K_C + C_s}$	Rate of Biodegradation in Biofilm
4.3	$J _{x=x_{AB}} = K_L \left(\frac{C_g}{HN} - C_I \right)$	Contaminant flux at the air/biofilm interface
4.4	$K_L \left(\frac{C_g}{HN} - C_I \right) = D_{Biofilm} \frac{dC_g}{dx} \Big _{x=x_{AB}}$	Assuming that the gas velocity with no flow condition is small in comparison with u_g and equating the fluxes at the air-biofilm interface
4.5	$\frac{1}{K_L} = \frac{1}{k_l} + \frac{1}{HNk_g}$	Overall mass transfer coefficient in the liquid phase (K_L) written in terms of the individual gas and liquid phase mass transfer coefficients, determined using standard correlations (Treybal, 1980)
4.6	$C_g = HNC_I - \frac{D_{Biofilm} HNkX_f}{K_L u_g} \left(\frac{C_I}{K_C + C_I} \right)$	Interfacial concentration obtained by combining equations (4.1), (4.3) and (4.4)
4.7	$u_g \frac{dC_g}{dh} = A_s D_{Biofilm} \frac{dC}{dx} \Big _{x=x_{AB}}$	Mass Balance along the height of the biofilter bed
4.8	$E = \frac{F_1 \tau k}{C_g^i \varepsilon} - \frac{F_2 k}{C_g^i} \ln \left(\frac{K_C HN + C_g^i}{K_C HN + C_g^o} \right) - \frac{(HNK_C - F_2 k)}{C_g^i} \ln \frac{C_g^i}{C_g^o}$ $F_1 = \frac{A_s D_{Biofilm} X_f}{u_g}; F_2 = \frac{X_f D_{Biofilm} HN}{K_L u_g}$	Differentiating equation (4.6), substituting into equation (4.7), and integrating from the biofilter inlet to the outlet

Nomenclature

A	specific area of the peat/compost particle (m^2m^{-3})
A_s	surface area of biomedica per unit volume of packed-bed (m^{-1})
b	contaminant velocity with no flow condition (ms^{-1})
B_{EC}	biofilter elimination capacity media factor (m^{-1})
$B_{\Delta P}$	biomedica pressure drop factor (m)
C	concentration of contaminant (gm^{-3})
Ca	capillary number (-)
C_b	bulk gas-phase concentration of contaminant (kgm^{-3})
C_f	gas-phase contaminant concentration at air/biofilm interface (kgm^{-3})
C_D	empirical friction factor for biomedica
C_g	gas-phase contaminant concentration (kgm^{-3})
C_{in}, C_g^i	Inlet gas concentration of contaminant (kgm^{-3})
C_g^o	concentration of contaminant in exit gas from biofilter (kgm^{-3})
C_I	interfacial contaminant concentration in biofilm (kgm^{-3})
C_o	oxygen concentration in particle (kgm^{-3})
C_s	contaminant concentration in biofilm (kgm^{-3})
d_s	equivalent diameter of a sphere with the same surface area as a single packing media element (m)
D_{Biofilm}	Diffusivity of contaminant in biofilm ($\text{m}^2\cdot\text{s}^{-1}$)
D_e	effective diffusivity of contaminant in particle (m^2s^{-1})
D_{e_o}	effective diffusivity of oxygen in particle (m^2s^{-1})
D_g	gas-phase diffusivity of contaminant (m^2s^{-1})
D_l	liquid-phase diffusivity of contaminant (m^2s^{-1})
E	fractional removal efficiency of biofilter (-)
E_o	characteristic energy of adsorption of a reference compound (Jmol^{-1})
EC_{Max}	maximum elimination capacity of biofilter when $E = 1$ ($\text{gm}^{-3}\text{s}^{-1}$)
f_{OC}	fraction of organic carbon in biomedica (-)
F_1	factor in biofilter efficiency, equation (4.8)
F_2	factor in biofilter efficiency, equation (4.8)
g	gravitational constant (ms^{-2})

h	direction along biofilter height (m)
H	height of biofilter bed (m)
HN	Dimensionless Henry's Law constant for contaminant (-)
J	contaminant flux ($\text{gm}^{-2}\text{s}^{-1}$)
k	Monod's maximum specific growth rate (s^{-1})
k_g	gas-phase mass transfer coefficient (ms^{-1})
k_l	liquid-phase mass transfer coefficient (ms^{-1})
K	maximum contaminant biodegradation rate = kX_f/Y
K_C	half velocity constant (kgm^{-3})
K_{CW}	half velocity constant for water (g water/g dry media)
K_d	hydrophobic partitioning constant (Lkg^{-1})
K_g	Overall gas-phase mass transfer coefficient (ms^{-1})
K_L	overall liquid-phase mass transfer coefficient (ms^{-1})
K_{OC}	hydrophobic partitioning constant normalized by organic carbon fraction (Lkg^{-1})
L_f	Biofilm thickness (μm)
MW_s	molecular weight of contaminant (g.mole^{-1})
P	total gas pressure (Pa)
P/P_o	partial pressure (kPa)
$q(C)$	total sorption of contaminant by biomedial
q'	adsorbed volume (m^3)
q'_{\max}	maximum sorption capacity (cm^3g^{-1})
$q_p(C)$	hydrophobic partitioning of contaminant to biomedial from aqueous phase (μgkg^{-1})
$q_{ad}(C)$	physical adsorption of contaminant on biomedial's surface (μgkg^{-1})
Q	Gas flow rate through biofilter (m^3s^{-1})
r	distance in radial direction
R	radius of particle
R_B	rate of biodegradation of contaminant in particle ($\text{gm}^{-3}\text{s}^{-1}$)
R_{Bo}	rate of oxygen consumption in particle due to contaminant biodegradation ($\text{gm}^{-3}\text{s}^{-1}$)
r_{observed}	actual measured reaction rate ($\text{kgm}^{-3}\text{s}^{-1}$)
$r_{\text{bulkconditions}}$	reaction rate determined at bulk conditions ($\text{kgm}^{-3}\text{s}^{-1}$)
R	ideal gas constant ($\text{Jmol}^{-1}\text{K}^{-1}$)

$R_{\text{Slough-off}}$	rate of biomass slough-off from the media's surface ($\text{kgm}^{-2}\text{s}^{-1}$)
S_R	residual saturation of biomedial packed bed (-)
T	absolute temperature (K)
u_g	empty-bed gas velocity in biofilter (ms^{-1})
V	Liquid flow rate per unit cross-sectional area of biofilter ($\text{gpm}\cdot\text{ft}^{-2}$)
V_{Bed}	Volume of biomedial in biofilter (m^3)
W	water content of media (g water/ g dry media)
W_i	critical water content below which irreversible loss of biodegradative capacity occurs (g water/g dry media)
W_o	original water content of media (g water/g dry media)
W_p	water content above which a water film appears outside particle (g water/g dry media)
W_{max}	water content when free drops of water appear within the media (g water/g dry media)
X_f	Biofilm density (kgm^{-3})
x	direction along biofilm thickness (m)
x_{AB}	position at air/biofilm interface
Z	dimension along height of biofilter bed (m)

Greek

β	stoichiometric ratio of oxygen consumption and contaminant biodegradation (-)
β_i	ratio of adsorption energies between the sorbate of interest and a reference compound
ε	Void fraction of biofilter packed-bed
ε_d	differential work of adsorption
μ_g	gas viscosity ($\text{kgm}^{-1}\text{s}^{-1}$)
ρ_f	fluid density (kgm^{-3})
ρ_g	gas density (kgm^{-3})
ρ_l	liquid density (kgm^{-3})
η	Biofilm Effectiveness Factor
σ	liquid surface tension (Nm^{-1})
τ	Empty-bed gas-phase residence time (s)
τ_s	shear stress on the biofilm's surface due to liquid flow (Nm^{-2})
θ	contact angle (degrees)
ΔP	gas-phase pressure drop across biofilter bed (Pa)

Figure 1. Schematic of Diffusive and Convective Support Media in Biofiltration: (a) Non-adsorptive Diffusive ; (b) Adsorptive Diffusive, with back-diffusion of contaminant from the media's surface into the biofilm; and (c) Convective, with gas flow through the biofilm and porous support media.

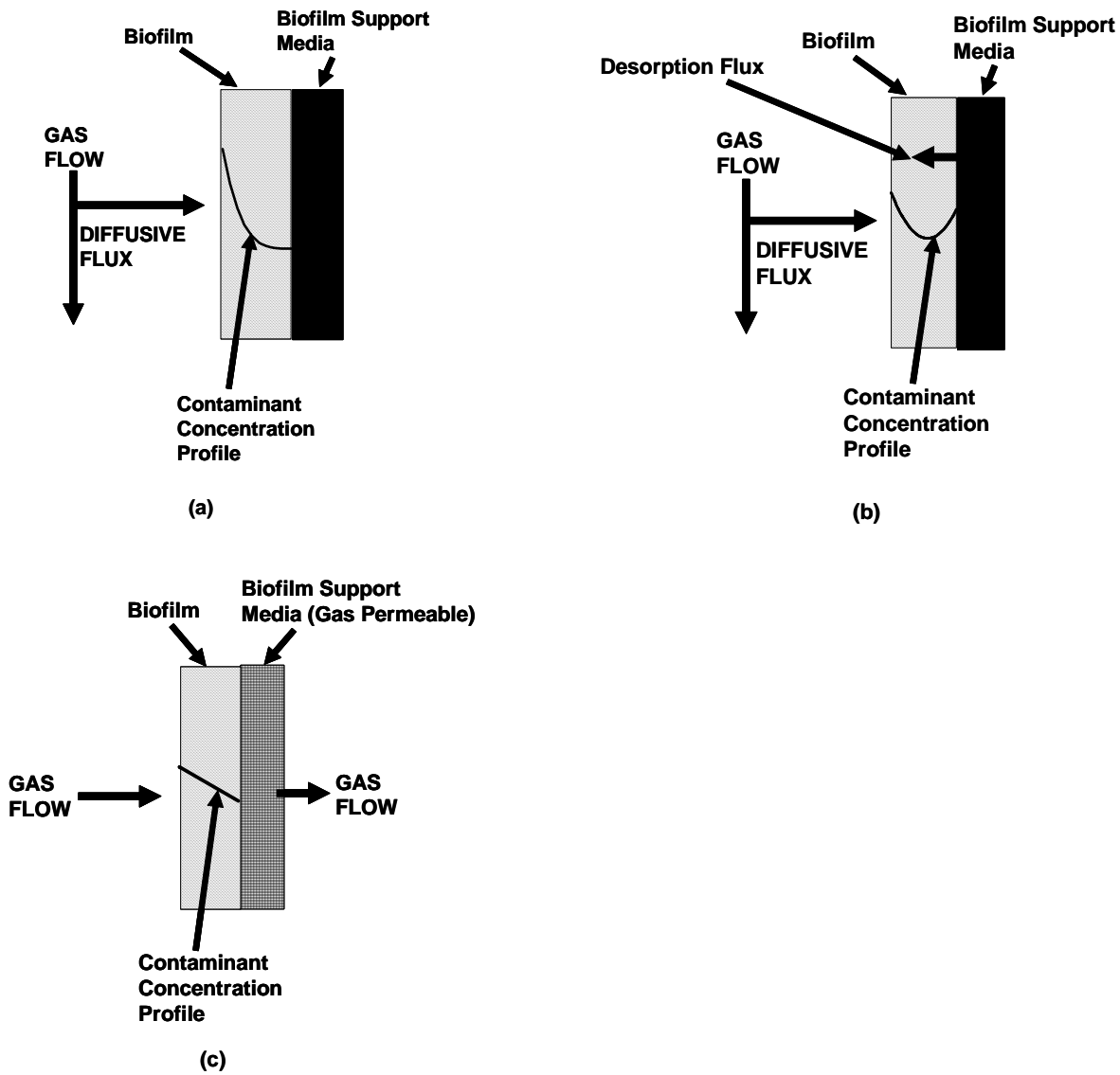


Figure 2. Biomedia surface with attached biofilm.

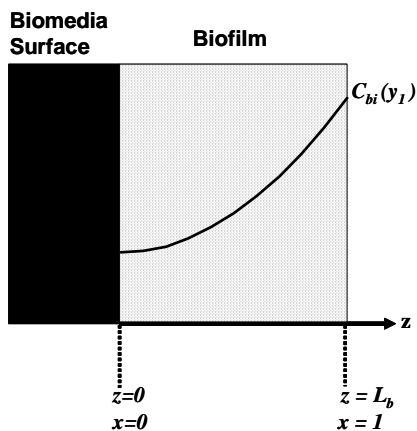


Figure 3. Plot of Biofilm Effectiveness Factor versus the Normalized contaminant concentration, and as a function of Thiele's Modulus ($\sqrt{\alpha}$).

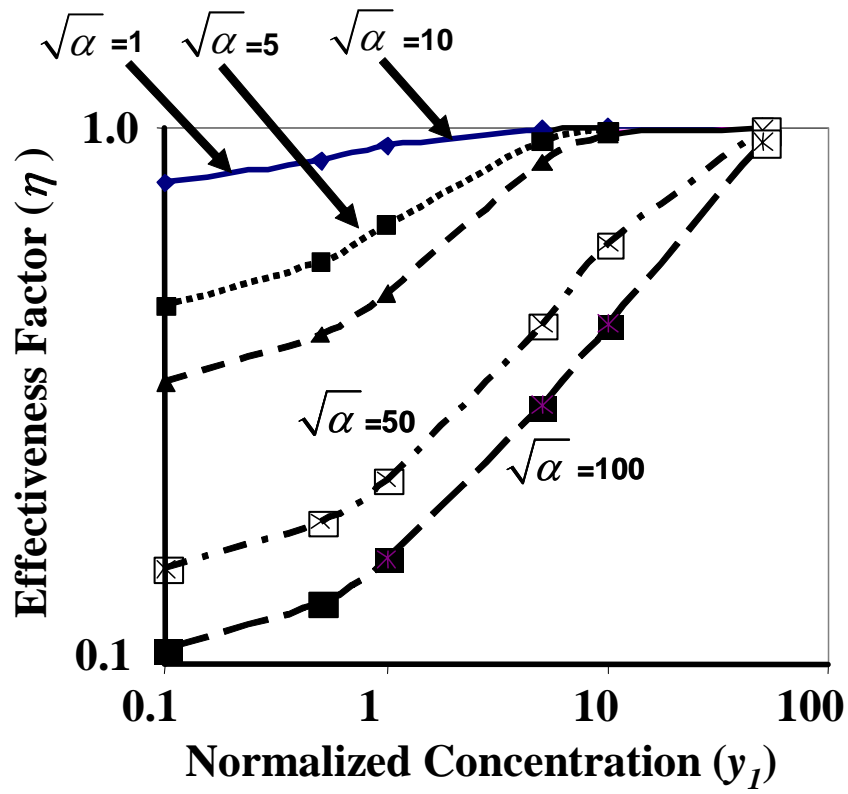


Figure 4. Effect of Water Content on Biofilter Removal Efficiency.

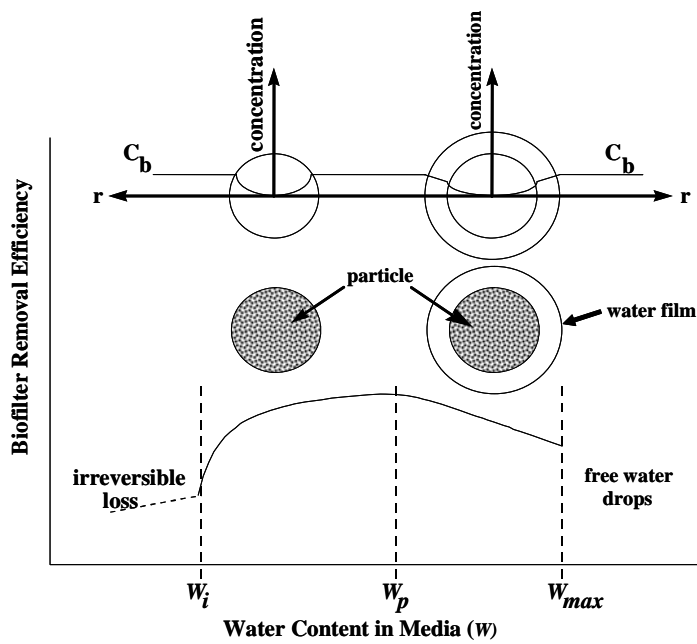


Figure 5. Biomass Slough-off Rate versus the Liquid Flow Rate in the Biofilter.

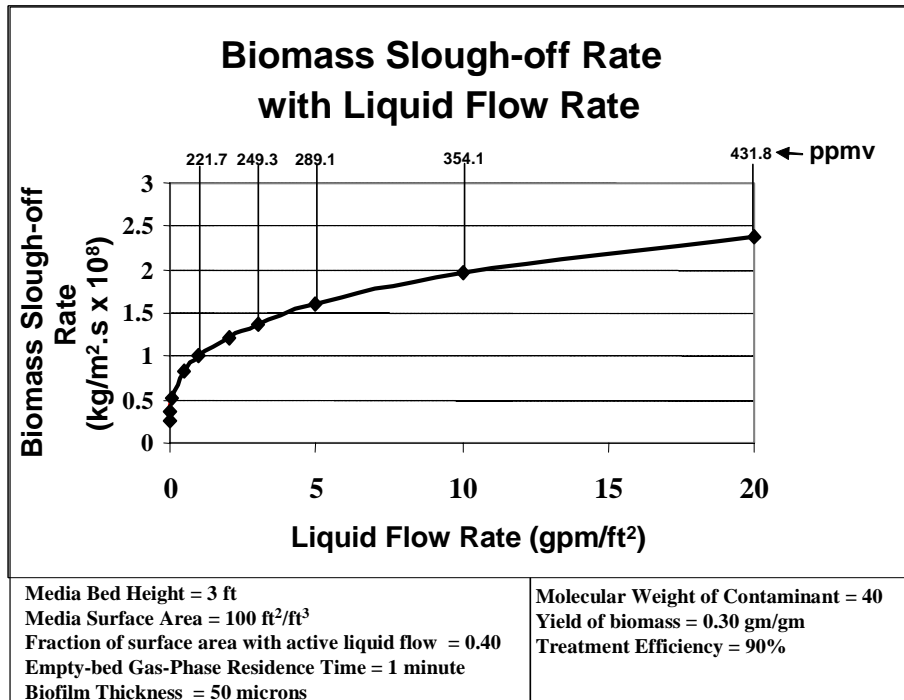


Figure 6. Plot of Maximum Elimination Capacity and Minimum Pressure Drop Biomeia Factors versus the Nominal Size.

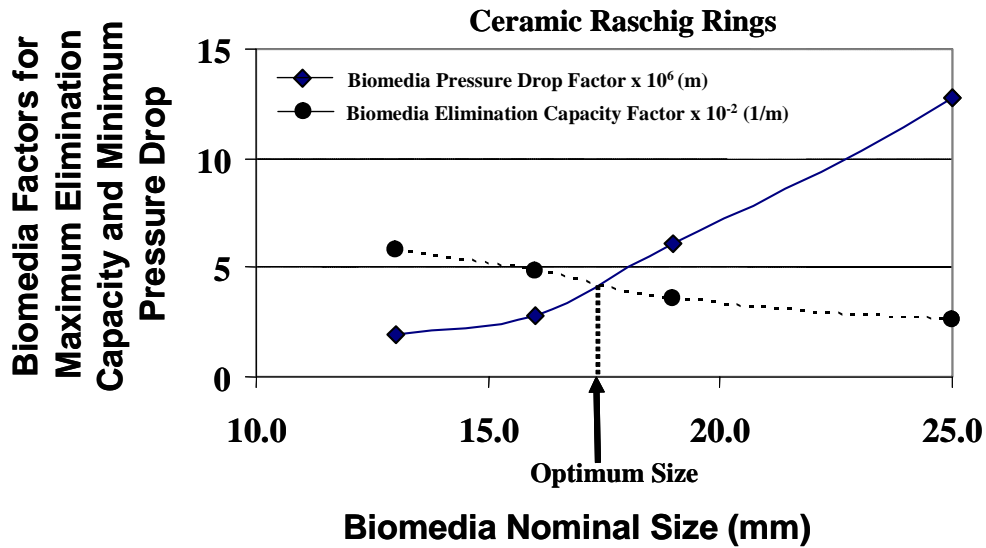


Figure 7. Residual Bed Saturation and Static Water Holdup in the Biofilter Bed for two different kinds of Packings.

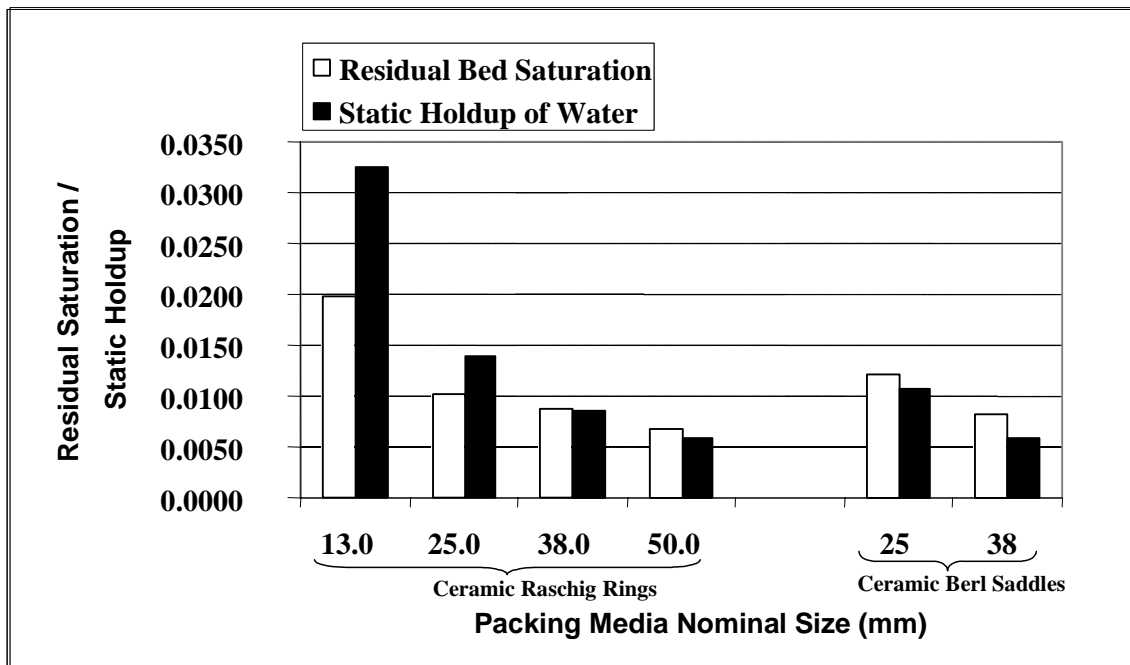


Figure 8. Schematic of the experimental system for studying different kinds of Biomedica.

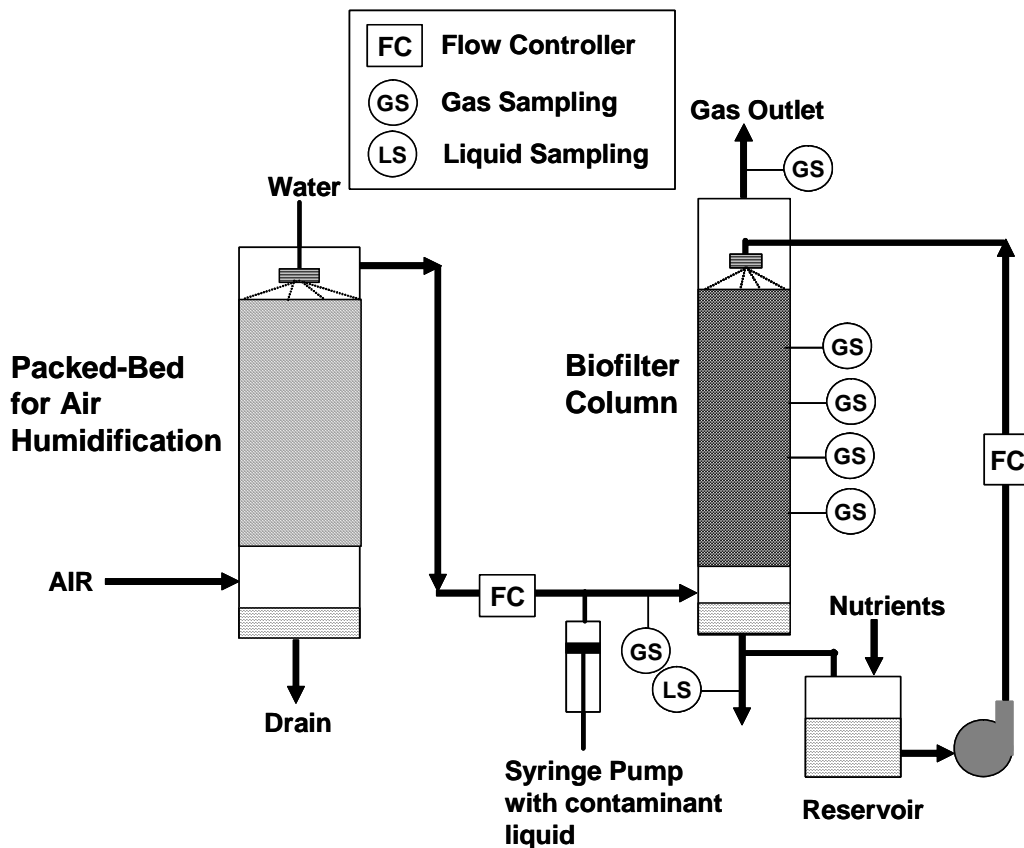


Figure 9. Iso-pentane outlet concentration as a function of gas-phase residence time (empty bed) for different biomedia.

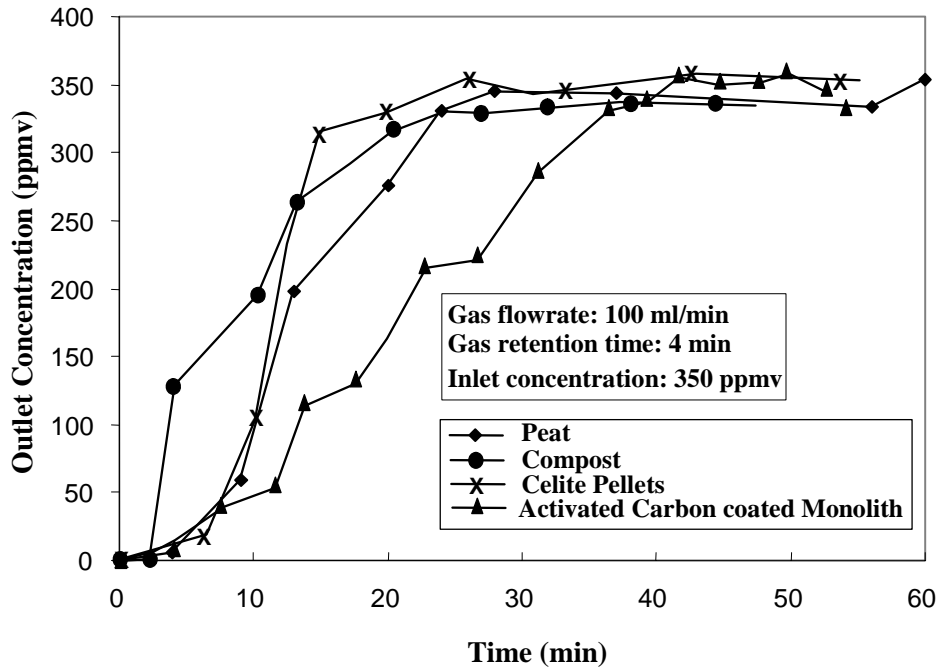


Figure 10. Effect of water content on removal efficiency of iso-pentane in peat and compost biofilters.

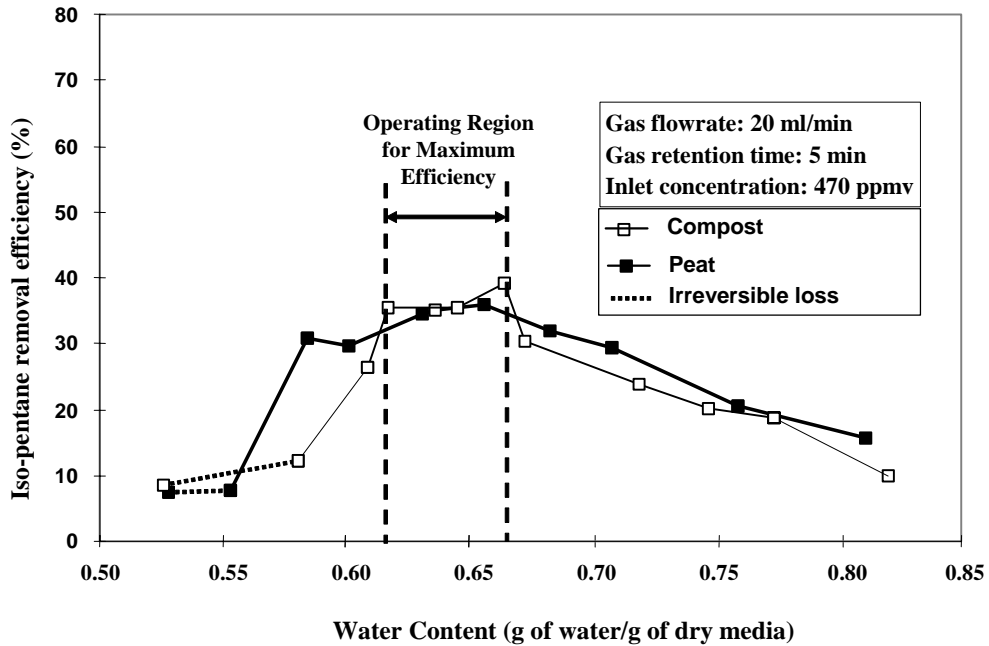


Figure 11. Comparison of different biomedica in terms of the maximum elimination capacity for iso-pentane.

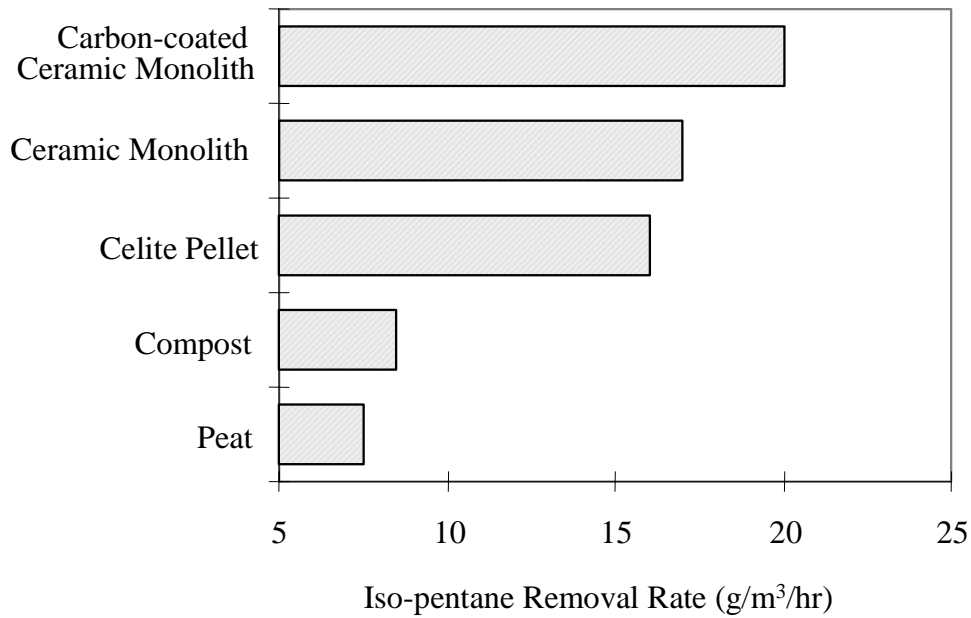


Figure 12. Monolith support media used in biofilter: (a) Diffusive, with gas entering and exiting through the straight passages; and (b) Convective, with gas entering and then flowing through the biofilms and porous walls of the monolith, by alternate blocking of passages in the top and bottom surfaces of the media.

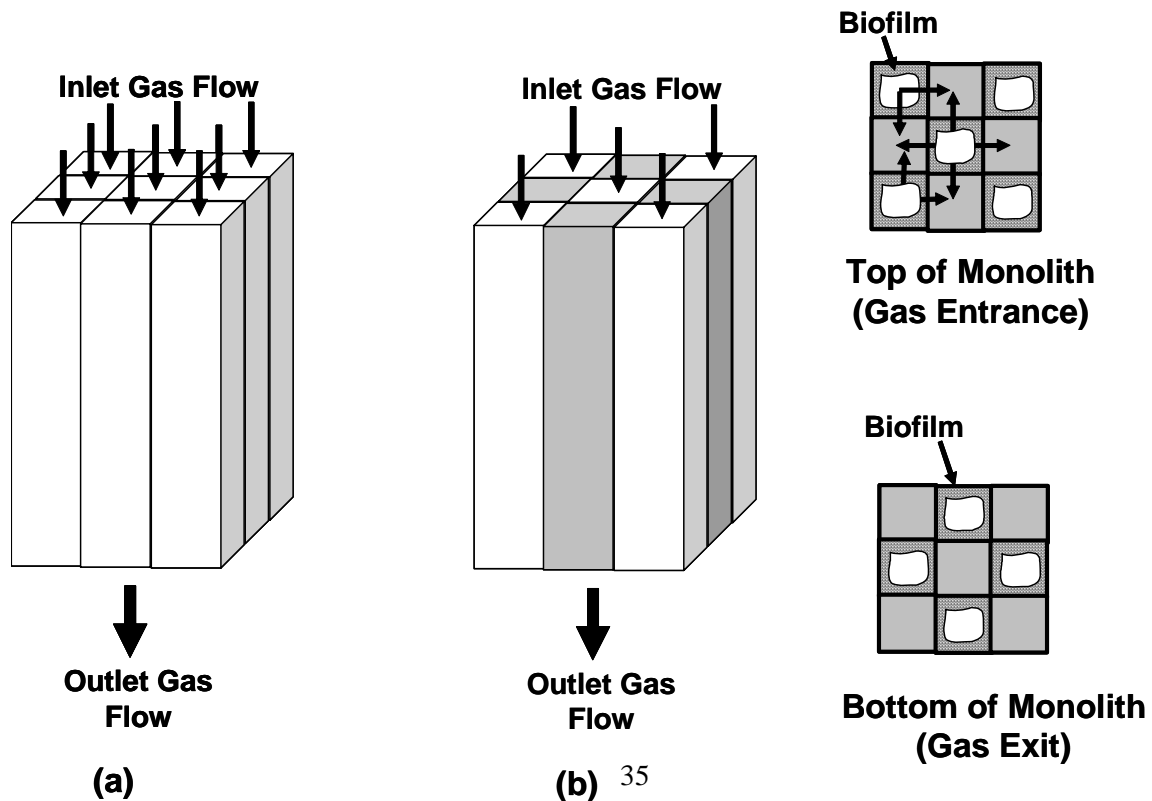


Figure 13. Removal Capacity of Toluene in a Diffusive and Convective Monolith Support Media Biofilter as a function of inlet concentration. The straight lines are model fits.

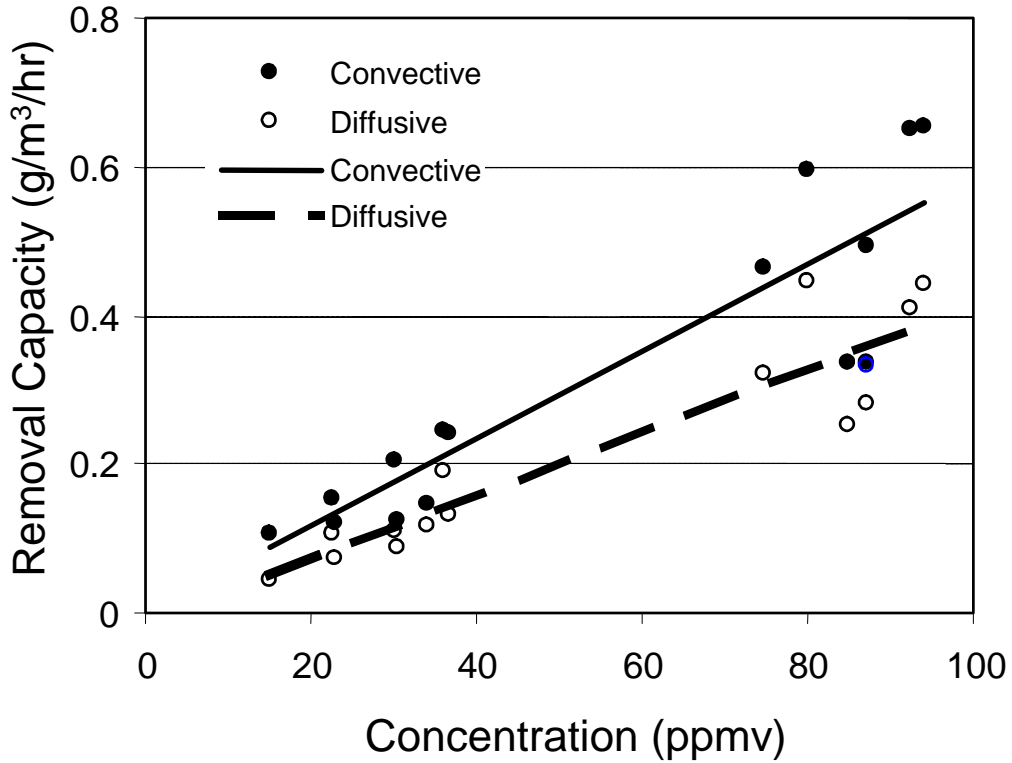


Figure 14. Exit concentration of toluene as a function of time in a silica gel bead encapsulated biomass biofilter, operated in batch mode.

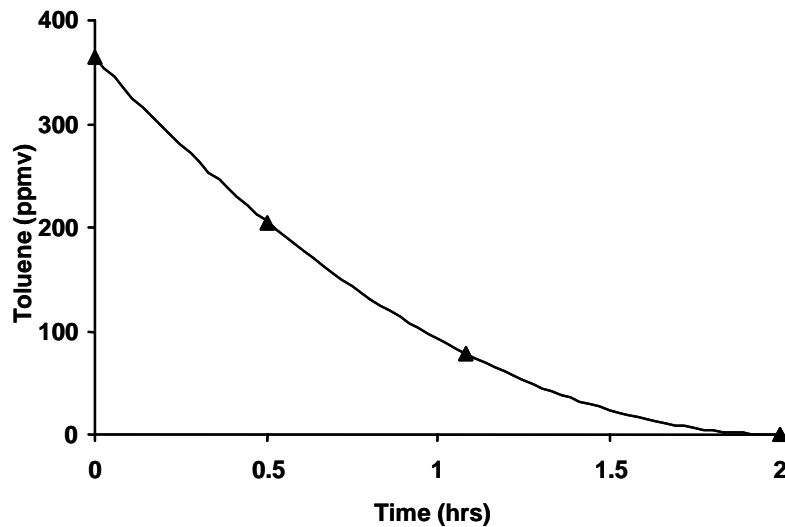


Figure 15. Concentration of acetate (liquid phase) and perchloroethylene (PCE) in the gas phase of a silica gel bead encapsulated biomass biofilter, operated in batch mode.

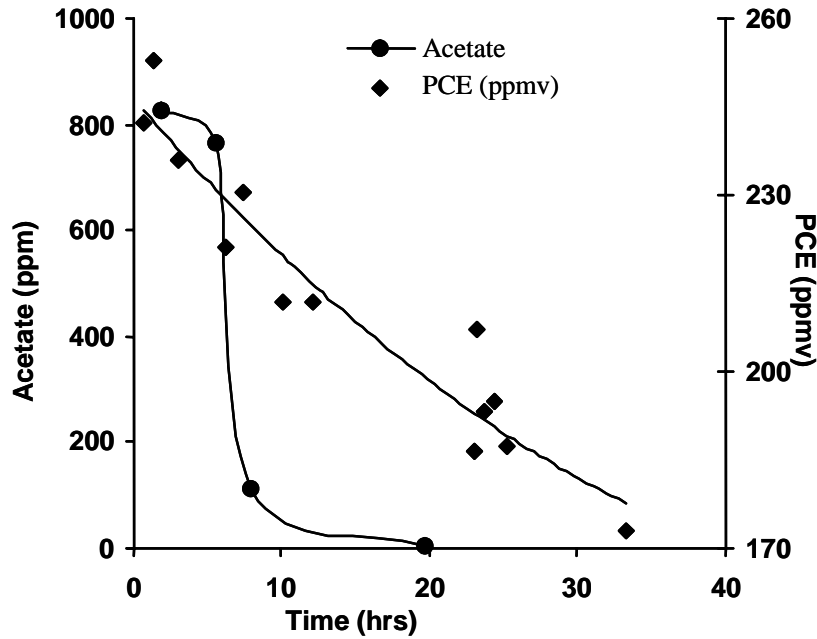


Figure 16. Schematic showing the mechanism of PCE degradation within the anoxic and aerobic zones that simultaneously co-exist within the gel bead.

